

**ornl**



3 4456 0358236 2

ORNL/TM-11739

**OAK RIDGE  
NATIONAL  
LABORATORY**

**MARTIN MARIETTA**

**Evaluation of Weldments in  
Type 21-6-9 Stainless Steel for  
Compact Ignition Tokamak  
Structural Applications**

**Phase I**

D. J. Alexander  
G. M. Goodwin  
E. E. Bloom

OAK RIDGE NATIONAL LABORATORY  
CENTRAL RESEARCH LIBRARY  
CIRCULATION SECTION  
4300N ROOM 575  
**LIBRARY LOAN COPY**  
DO NOT TRANSFER TO ANOTHER POSITION  
If you wish someone else to see this  
report, send in memo with report and  
the library will arrange a loan.  
60871448-1739

MANAGED BY  
MARTIN MARIETTA ENERGY SYSTEMS, INC.  
FOR THE UNITED STATES  
DEPARTMENT OF ENERGY

This report has been reproduced directly from the best available copy.

Available to DOE and DOE contractors from the Office of Scientific and Technical Information, P.O. Box 62, Oak Ridge, TN 37831; prices available from (615) 576-8401, FTS 626-8401.

Available to the public from the National Technical Information Service, U.S. Department of Commerce, 5255 Port Royal Rd., Springfield, VA 22161.

This report was prepared as an account of work sponsored by an agency of the United States Government. Neither the United States Government nor any agency thereof, nor any of their employees, makes any warranty, express or implied, or assumes any legal liability or responsibility for the accuracy, completeness, or usefulness of any information, apparatus, product, or process disclosed, or represents that its use would not infringe privately owned rights. Reference herein to any specific commercial product, process, or service by trade name, trademark, manufacturer, or otherwise, does not necessarily constitute or imply its endorsement, recommendation, or favoring by the United States Government or any agency thereof. The views and opinions of authors expressed herein do not necessarily state or reflect those of the United States Government or any agency thereof.

ORNL/TM-11739  
Distribution  
Category UC-424

Metals and Ceramics Division

EVALUATION OF WELDMENTS IN TYPE 21-6-9 STAINLESS  
STEEL FOR COMPACT IGNITION TOKAMAK  
STRUCTURAL APPLICATIONS

PHASE I

D. J. Alexander  
G. M. Goodwin  
E. E. Bloom

Date Published: June 1991

NOTICE: This document contains information of a preliminary nature. It is subject to revision or correction and therefore does not represent a final report.

Prepared for the  
DOE Office of Fusion Energy  
61 30 52 12 4

Prepared by the  
OAK RIDGE NATIONAL LABORATORY  
Oak Ridge, Tennessee 37831-6285  
managed by  
MARTIN MARIETTA ENERGY SYSTEMS, INC.  
for the  
U.S. DEPARTMENT OF ENERGY  
under Contract DE-AC05-84OR21400



3 4456 0358236 2

100

1

2

3

4

5

## CONTENTS

LIST OF TABLES . . . . .	v
LIST OF FIGURES . . . . .	vii
ABSTRACT . . . . .	1
INTRODUCTION . . . . .	1
MATERIALS . . . . .	3
WELDING . . . . .	3
EXPERIMENTAL PROCEDURE . . . . .	5
RESULTS . . . . .	8
DISCUSSION . . . . .	22
CONCLUSIONS . . . . .	26
ACKNOWLEDGMENTS . . . . .	27
BIBLIOGRAPHY . . . . .	28



LIST OF TABLES

Table 1. Chemical analyses (wt %) of materials for the Compact Ignition Tokamak weldment study . . . . .	4
Table 2. Phase I weldments . . . . .	5
Table 3. Results of base metal tensile tests . . . . .	9
Table 4. Results of subsize weld metal tensile tests . . . . .	10
Table 5. Base metal Charpy tests . . . . .	12
Table 6. Weld metal Charpy tests . . . . .	13



## LIST OF FIGURES

Fig. 1. View of weldment showing specimen orientations . . . . .	6
Fig. 2. Gleeble thermal cycle for fusion weld in thick stain- less steel plate . . . . .	7
Fig. 3. Comparison of the average yield and ultimate tensile strengths for the type 21-6-9 base metals and the weld filler metals (top: room temperature; bottom: 77 K) . . . . .	11
Fig. 4. A comparison of the average Charpy impact energies for the type 21-6-9 base metals and the weld filler metals at room tempera- ture and at 77 K . . . . .	14
Fig. 5. Weld G25 with the 21-6-9 filler metal: (a) macroscopic view of weld, (b) low-magnification view of weld metal, and (c) higher magnification view showing ferrite phase in an austenitic matrix . . . . .	15
Fig. 6. Weld G17 with Nitronic 40W filler metal: (a) macro- scopic view of weld, (b) low-magnification view of weld metal, and (c) higher magnification view showing ferrite phase in an austenitic matrix . . . . .	16
Fig. 7. Weld G20 with Nitronic 35W filler metal: (a) macro- scopic view of weld, (b) low-magnification view of weld metal, and (c) higher magnification view showing ferrite phase in an austenitic matrix . . . . .	17
Fig. 8. Weld G19 with Inconel 82 filler metal: (a) macroscopic view of weld, (b) low-magnification view of weld metal showing iso- lated porosity and lack of fusion in the weld metal, and (c) higher magnification of weld metal showing fully austenitic weld . . . . .	18
Fig. 9. Weld G28 with Inconel 182 filler metal: (a) macro- scopic view of weld, (b) low-magnification view of weld metal, (c) higher magnification view, and (d) view of edge of weld showing lack of fusion at fusion line . . . . .	19
Fig. 10. Weld G18 with Inconel 625 filler metal: (a) macro- scopic view of weld, (b) low-magnification view of weld metal, and (c) higher magnification of weld metal showing fully austenitic weld . . . . .	20

Fig. 11. Weld G27 with Inconel 625 PLUS filler metal:  
 (a) macroscopic view of weld, (b) low-magnification view of weld metal showing lack of fusion in the weld metal, and (c) higher magnification of weld metal showing fully austenitic weld . . . . . 21

Fig. 12. Type 21-6-9 base metal: (a) base metal from forging from weld G17 (note austenitic matrix with twins in grains and occasional regions of ferrite), (b) base metal from 100-mm plate from weld G20, and (c) heat-affected zone from weld G20 (note fine structure in austenite grains and coarser carbides on grain boundaries near weld fusion line) . . . . . 23

Fig. 13. Fractographs of Nitronic 40W weld metal Charpy impact specimen tested at room temperature: (a) low-magnification view and (b) higher magnification showing ductile, dimpled fracture . . . . . 24

Fig. 14. Fractographs of Nitronic 40W weld metal Charpy impact specimen tested at 77 K: (a) low-magnification view showing stepped surface and (b) higher magnification showing flat regions joined by tear ridges . . . . . 25

EVALUATION OF WELDMENTS IN TYPE 21-6-9 STAINLESS STEEL FOR COMPACT  
IGNITION TOKAMAK STRUCTURAL APPLICATIONS - PHASE I\*

D. J. Alexander, G. M. Goodwin, and E. E. Bloom

ABSTRACT

Primary design considerations for the Compact Ignition Tokamak toroidal field-coil cases are yield strength and toughness in the temperature range from 77 to 300 K. Type 21-6-9 stainless steel, also still known by its original Armco Steel Company trade name Nitronic 40, is the proposed alloy for this application. It has high yield strength and usually adequate base metal toughness, but weldments in thick sections (i.e., >25 mm) have not been adequately characterized in terms of mechanical properties or hot-cracking propensity.

In this study, weldability of the alloy in heavy sections and the mechanical properties of the resultant welds were investigated including tensile yield strength and Charpy V-notch toughness at 77 K and room temperature. Weldments were made in four different base metals using seven different filler metals. None of the weldments showed any indication of hot-cracking problems. All base metals, including weldment heat-affected zones, were found to have adequate strength and impact toughness at both test temperatures. Weld metals, on the other hand, except ERNiCr-3 (i.e., Inconel 82) and ENiCrFe-3 (i.e., Inconel 182) had impact toughnesses of less than 67 J (50 ft-lb) at 77 K. Inconel 82 had an average weld metal impact toughness of over 135 J (100 ft-lb) at 77 K, and although its strength at 77 K is less than that of type 21-6-9 base metal, at this point it is considered to be the first-choice filler metal. Phase II of this program will concentrate on composition refinement and process/procedure optimization for the generic ERNiCr-3 composition and will generate a design data base for base and weld metal, including tensile, fracture toughness, and crack growth rate data.

---

INTRODUCTION

Type 21-6-9 stainless steel is one alloy in a family of nitrogen-strengthened, high-manganese austenitic alloys possessing high yield

---

\*Research sponsored by the Office of Fusion Energy, U.S. Department of Energy, under contract DE-AC05-84OR21400 with Martin Marietta Energy Systems, Inc.

strengths and usually adequate base metal toughnesses. It has been selected as the primary structural material for the Compact Ignition Tokamak (CIT) toroidal field-coil cases that will operate from liquid nitrogen (77 K) to room temperature. These alloys were developed by Armco Steel Company for good corrosion resistance and elevated temperature strength, but their excellent mechanical properties make them attractive for other applications. Armco's original trade name for what has generally become type 21-6-9 is Nitronic 40; when the alloy has been given an electroslag remelt treatment during its production, it is typically called type 21-6-9--referring to its nominal composition of 21Cr-6Ni-9Mn.

Type 21-6-9 is typically used only in sheet thickness; weldments in thick sections (i.e., >25 mm) are rarely produced. For the CIT, 100-mm-thick sections are anticipated. In autogenous welds porosity can be a problem because of the high base metal nitrogen content. Slow travel and high heat input are recommended to minimize this potential problem. For thicker section welds, modified composition filler metal is suggested and, even then, porosity and poor wetting can occur because of base metal dilution. The Nitronic "type W" filler metals have reduced nitrogen and a balanced chromium:nickel ratio; this ensures that enough ferrite will be in the weld deposit to avoid hot cracking. As a result of these modifications, weld metal usually has somewhat different mechanical properties than base metal, and one might anticipate that delta ferrite in the weld metal would reduce toughness at cryogenic temperatures.

In some austenitic alloys, the weldment heat-affected zone (HAZ) can show mechanical properties significantly different from the base metal. The part of the HAZ nearest the fusion line undergoes a thermal excursion that reaches the melting point. Grain growth occurs in the higher temperature regions, and precipitation of nitrides, carbides, or other phases can occur.

The type of welding process used can affect weld metal strength and toughness. Smaller substructure size [e.g., gas tungsten arc (GTA) versus submerged arc] usually gives higher strength, while higher inclusion count (e.g., shielded metal arc versus gas tungsten arc) will typically decrease toughness. This investigation assesses the mechanical properties, particularly yield strength and impact toughness at 77 K and room

temperature, of various weldments in thick sections (i.e., a minimum of 25 mm) of type 21-6-9 stainless steel. A bibliography of relevant references is included at the end of this report.

### MATERIALS

Four different base metals were included in this study; Table 1 depicts their chemical analyses. Three are type 21-6-9 and one, a 100-mm-thick, hot-rolled slab, is Nitronic 40. Both the Nitronic 40 slab and the 175-mm-thick, type 21-6-9, hot-rolled slab have subsequently been rolled to 50-mm-thick plate and will be used in Phase II of this program. Both slabs were characterized in both the as-received (hot-rolled) and annealed condition. Annealing was performed at 1065°C (1950°F) followed by water quench. Pieces 50 mm thick were sawed from each slab for welding.

Seven weld filler metals were included in the program; Table 1 lists their compositions. Six were added as cold filler wire using the argon-shielded GTA welding process, and ENiCrFe-3 (i.e., Inconel\* 182) is a coated electrode for use with the shielded metal arc process. ERNiCrMo-3 (i.e., Inconel 625) is the Armco-recommended filler metal to use if 35W or 40W are not appropriate for some reason. ERNiCr-3 (i.e., Inconel 82) is a universal filler metal widely used to join a variety of nickel-based alloys and numerous dissimilar metal combinations, including austenitics to ferritics. Type 21-6-9 filler is essentially a matching composition weld metal for type 21-6-9 base plate. Inconel 625 PLUS is a modified Inconel 625 composition recently introduced by Carpenter Technology Corporation.

### WELDING

Seven welds were made; Table 2 lists the base metal and filler metal combinations. All the base materials were prepared with a double-groove, butt-weld geometry. For the 25-mm-thick, type 21-6-9 plate, a double-V joint design was used with a 45° included angle, a 1.5-mm root face, and a

---

\*Inconel is a registered trademark of Huntington Alloys, Inc., Huntington, West Virginia.

Table 1. Chemical analyses (wt %) of materials for the Compact Ignition Tokamak weldment study

Material		C	Mn	Si	P	S	Cr	Ni	Mo	Cu	Co	Al	Ti	Nb+Ta	W	Fe	N
Type 21-6-9 forging (25-mm thick)	nominal actual	0.08	8.0-10.0	1.0	0.060	0.030	19.0-21.5	5.5-7.5								Bal	0.15-0.4
Type 21-6-9 plate (22-mm thick)	nominal actual	0.08	8.0-10.0	1.0	0.060	0.030	19.0-21.5	5.5-7.5								Bal	0.15-0.4
Type 21-6-9 slab (175 mm)	nominal actual	0.08 0.027	8.0-10.0 8.76	1.0 0.41	0.060 0.015	0.030 0.001	19.0-21.5 19.85	5.5-7.5 7.31	0.24	0.09						Bal	0.15-0.4 0.27
Nitronic 40 slab (100 mm)	nominal actual	0.08 0.023	8.0-10.0 9.16	1.0 0.55	0.060 0.030	0.030 0.001	19.0-21.5 19.76	5.5-7.5 7.14	0.21	0.26						Bal	0.15-0.4 0.32
Nitronic 40W weld metal (in forging)	nominal 1.5-mm wire deposit	0.03 0.026	9.00 9.04	0.40 0.40			20.50 20.49	6.50 6.44	0.01	0.03							0.25 0.26
Nitronic 35W weld metal (in 100-mm slab)	nominal 1.5-mm wire deposit	0.05 0.041	12.0 12.70	0.40 0.46	0.007	0.006	18.00 17.96	5.00 4.95									0.15 0.17
Inconel 625 weld metal (in 25-mm plate)	nominal 1.5-mm wire deposit	0.10	0.50	0.50	0.02	0.015	20.0-23.0	58 min	8.0-10.0	0.50		0.40	0.40	3.15-4.15		5.0	
Inconel 82 weld metal (in 175-mm slab)	nominal 3-mm wire deposit	0.10 0.03	2.5-3.5 3.05	0.50 0.18	0.03 0.006	0.015 0.002	18.0-22.0 19.95	67 min 71.36		0.50 0.16			0.75 0.45	2.0-3.0 2.51		3.0 2.31	
Type 21-6-9 weld metal (in 25-mm plate)	nominal 1.1-mm wire deposit		9.00					21.00	6.0								
Inconel 625 PLUS weld metal (in 25-mm plate)	nominal 2.3-mm wire deposit	0.015 0.009	0.10 0.03	0.10 0.03	0.005 0.007	0.002 0.002	20.50 21.03	61.0 60.84	8.50 7.96		0.01 0.01	0.20 0.18	1.30 1.31	3.30 3.39		Bal 0.03	5.18
Inconel 182 weld metal (in 25-mm plate)	nominal 3-mm wire deposit	0.05 0.04	7.80 6.84	0.50 0.51		0.008 0.005	14.0 14.62	67.0 68.25		0.10 0.14		0.40 0.33	1.80 1.67			7.50 7.56	

Table 2. Phase I weldments

Weld	Description
G17	Ring-forging base metal with Nitronic 40W filler
G18	25-mm plate with Inconel 625 filler metal
G19	50-mm plate (cut from 175-mm plate) with Inconel 82 filler metal
G20	50-mm plate (cut from 100-mm plate) with Nitronic 35W filler metal
G25	25-mm plate with type 21-6-9 filler metal
G27	25-mm plate with Inconel 625 PLUS filler metal
G28	25-mm plate with Inconel 182 filler metal

3-mm root opening. For all other base materials, a double-U joint design was used with a 15° included angle, a 6-mm radius, a 1.5-mm root face, and a 3-mm root opening.

The GTA welds were made at 10- to 14-V direct current electrode negative (DCEN) and 125 to 200 A with pure argon shielding gas using a stringer bead technique. The 25-mm plates required 30 to 40 passes; the 50-mm plates, 90 to 100 passes. The Inconel 182 shielded metal-arc weld in 25-mm plate was made with 3-mm electrodes at 100 A and 23-V direct current electrode positive (DCEP). Eighteen passes completed the weld. Since subsequent sectioning would reveal any defects, inspection of all welds was visual only.

#### EXPERIMENTAL PROCEDURE

Test specimens for determining the mechanical properties were cut from the welds (see Fig. 1). To avoid the middle of the plate where the welds were thinnest and the dilution greatest, the specimens were centered in the weld metal and located near the top and bottom surfaces of the plates.

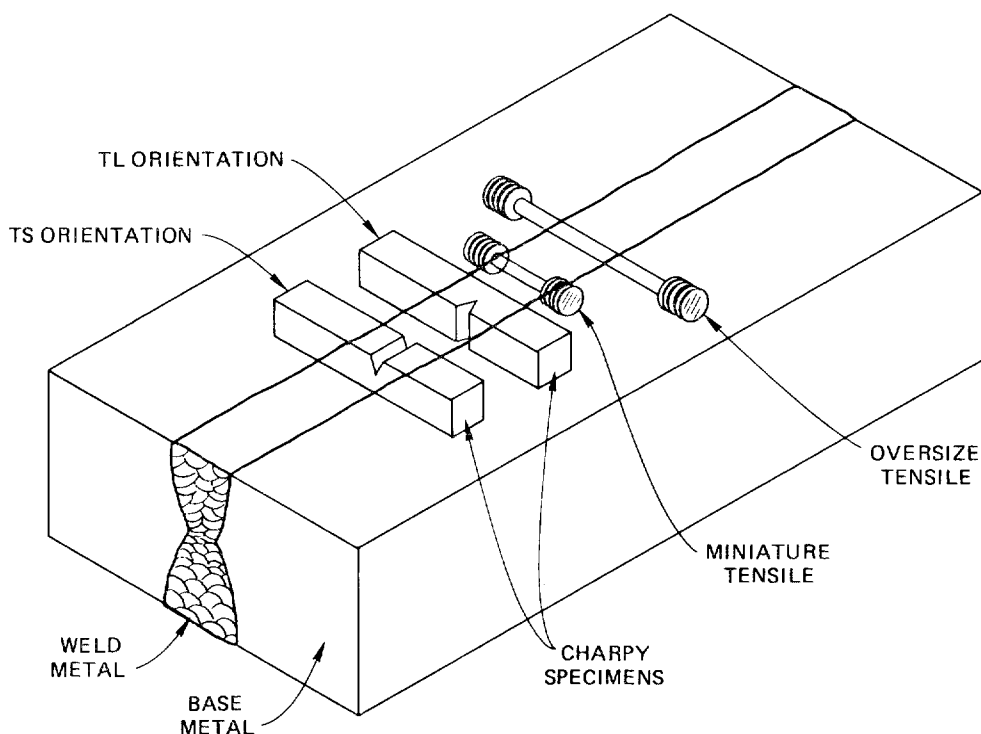


Fig. 1. View of weldment showing specimen orientations.

Two types of tensile specimens were tested. Oversize tensile specimens [i.e., gage length  $38.1 \times 5.1$  mm in diameter ( $1.5 \times 0.20$  in.)] traversed the entire weld and, thus, included base metal, HAZ, and weld metal. Testing of these specimens provided a qualitative demonstration of the relative strengths of these different zones and identified the weakest link in the compound structure. Miniature tensile specimens [i.e., gage length  $10.2 \times 2.5$  mm in diameter ( $0.40 \times 0.10$  in.)] were machined transverse to the weld. These specimens were small enough that the reduced diameter gage length was wholly contained in the weld metal.

Tensile testing was conducted on a screw-driven electromechanical test machine at a constant crosshead speed of  $4.2 \times 10^{-3}$  mm/s (0.01 in./min). This resulted in an initial strain rate of  $4.2 \times 10^{-4}$  s $^{-1}$  for the small specimens. Duplicate tests were conducted at room temperature and 77 K—the latter by immersing the specimen in a bath of liquid nitrogen contained in a vacuum Dewar flask. Load and crosshead displacement were recorded, and the 0.2% offset yield strength was derived from this record after

allowance for the test system compliance. Uniform and total elongations were measured from this load-displacement trace. Reduction of area was measured from the broken specimen halves.

Charpy specimens were tested at room temperature and at 77 K. The specimens were immersed in a bath of liquid nitrogen and then quickly transferred to the test machine with special tongs that centered the specimen on the test machine anvils. Two orientations of specimens were tested (Fig. 1): the TL specimens were notched so that the fracture would propa-gate in the direction of welding; the TS specimens, so that the fracture would propagate through the weld thickness.

The properties of the HAZ material were studied using simulated HAZ material produced on a Gleeble thermomechanical simulator, a device used to produce a bulk specimen with the same microstructure as that at a given location in the HAZ of a weldment. This is accomplished by exposing the specimen to a preprogrammed thermal cycle equivalent to that experienced by the subject HAZ location. Figure 2 shows a thermal cycle typical of a

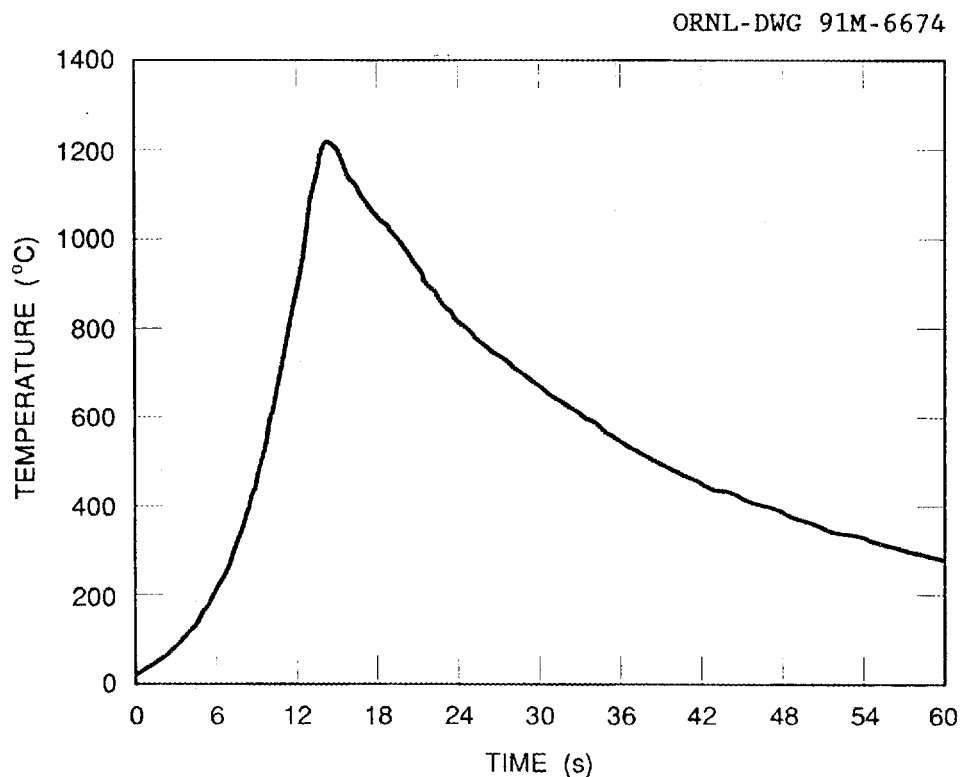


Fig. 2. Gleeble thermal cycle for fusion weld in thick stainless steel plate.

fusion weld in thick stainless steel plate. A peak temperature of 1200°C was used for these materials (roughly 50°C below the onset of melting); this represents a point near the fusion line of a weld. Square bar specimens, 12.5 × 12.5 × 75 mm long, were machined from each of the base materials and subjected to this thermal cycle; this was followed by machining into either Charpy V-notch specimens or reduced-section tensile specimens. Sections from the welds were metallographically polished and etched to allow the different microstructures to be examined.

## RESULTS

All the welds appeared to be sound and free of defects up on visual inspection after welding. No evidence of hot cracking was observed, but wetting was poor (as anticipated) because of dilution of the weld metal by the high nitrogen base metal.

The tensile data are presented in Tables 3 and 4 and are summarized in Fig. 3. At room temperature, all of the filler metals had yield strengths that exceeded the base metal. However, the strength of the base metal increased more than the weld metal from room temperature to 77 K; thus, at 77 K the yield strength of the Nitronic 35W, 40W, and the type 21-6-9 filler metals exceeded that of the base metal, while the Inconel 625, 625 PLUS, 82, and 182 filler metals were significantly weaker.

Close post-test examination of the oversize tensile specimens indicated that the HAZ was stronger than the base metal (at least at room temperature) since the diameter of the specimen in the HAZ area was greater than the base metal further from the weld. At 77 K, the deformation was largely limited to the weld metal, and the HAZ and base metal regions were unaltered. Fracture occurred in the weld metal for all of the specimens at either test temperature.

The impact energies are shown in Tables 5 and 6 and are summarized in Fig. 4. The impact toughnesses of the base metals are very high at room temperature. Although the toughnesses of the base metals drop at 77 K, they are still high. Except for Inconel 625, all the filler metals had good impact properties at room temperature. However, at 77 K the impact

Table 3. Results of base metal tensile tests

Material	Condition	Temperature (°C)	Strength (ksi)		Elongation (%)	
			Yield	Ultimate tensile	Uniform	Total
Ring forging	Base metal	22	52	105	20	28
			51	105	20	27
		-196	142	213	23	28
			141	211	23	27
	Gleebled	22	56	105	18	26
			58	107	19	28
	-196	136	214	20	23	
		136	215	21	24	
1-in. plate	Not known	22	54	106	21	28
			55	106	21	29
		-196	145	216	23	27
			146	215	21	28
4-in. plate	Quenched	22	70	108	50	72
			57	109	50	68
		-196	156	219	41	41
			153	218	38	38
	Hot rolled	22	56	110	48	61
			52	106	52	68
	-196	147	214	37	47	
		144	214	43	45	
7-in. plate	Quenched	22	56	104	49	64
			54	101	47	57
		-196	141	209	40	40
			131	211	56	67
	Hot rolled	22	46	100	52	69
			49	100	45	56
	-196	129	197	36	36	
		139	206	41	41	

Table 4. Results of subsize weld metal tensile tests

Material	Temperature (°C)	Strength (ksi)		Elongation (%)	
		Yield	Ultimate tensile	Uniform	Total
Nitronic 40W	22	76	103	18	27
		84	107	17	25
	-196	155	207	23	23
		150	187	11	11
Nitronic 35W	22	80	108	29	41
		92	113	20	36
	-196	171	214	21	21
		113	192	29	29
Type 21-6-9 filler	22	87	117	27	39
		81	113	25	36
	-196	174	230	31	31
		169	225	23	23
Inconel 625	22	74	117	26	27
		75	119	28	31
	-196	109	164	20	20
		105	162	17	17
Inconel 625 PLUS	22	72	116	34	39
		73	115	28	34
	-196	99	160	31	32
		103	162	30	31
Inconel 82	22	68	101	24	32
		73	106	27	34
	-196	119	149	16	26
		91	137	32	38
91		134	24	27	
99		140	22	28	
Inconel 182	22	58	91	27	34
		59	92	24	33
	-196	77	129	27	36
		76	132	35	44

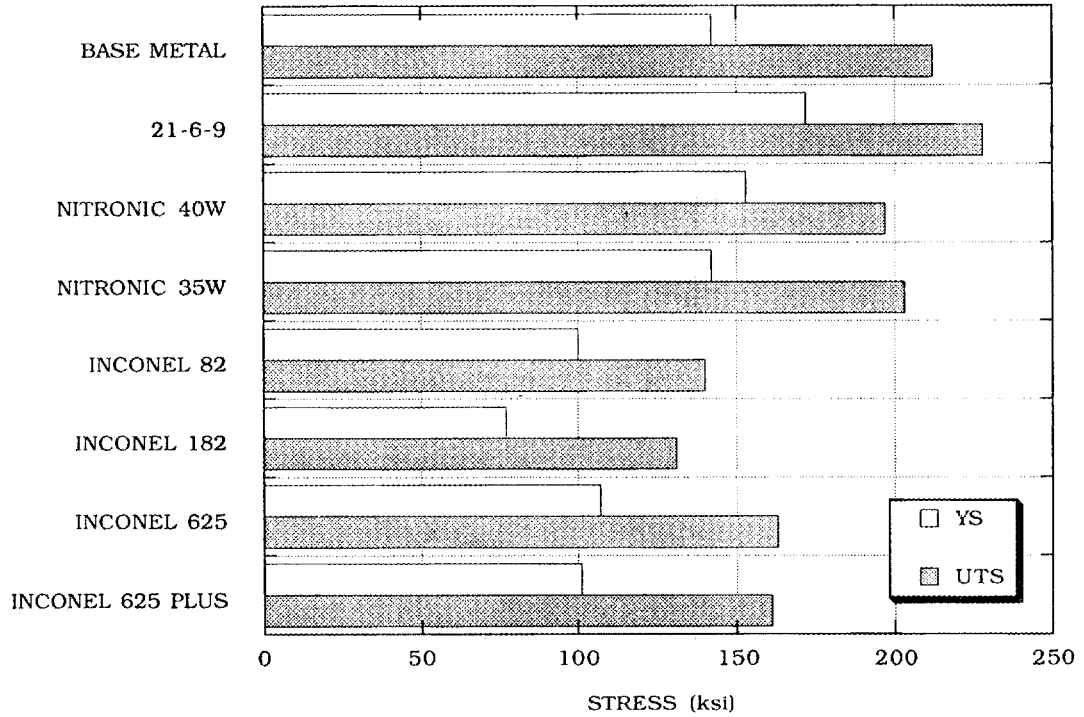
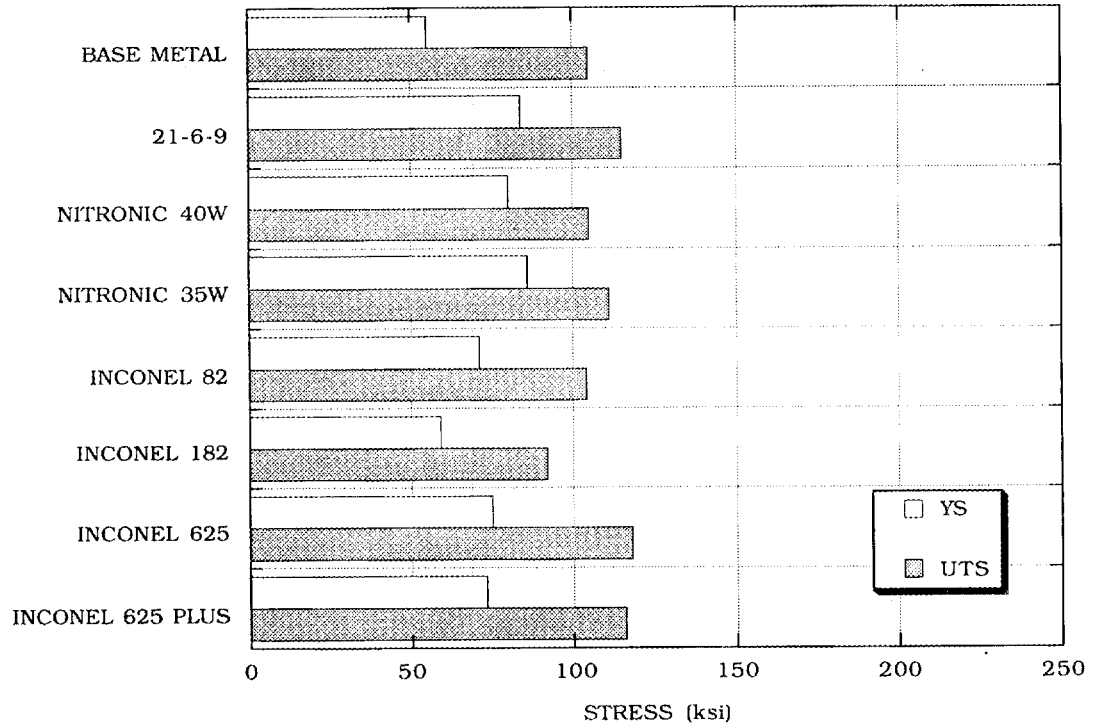


Fig. 3. Comparison of the average yield and ultimate tensile strengths for the type 21-6-9 base metals and the weld filler metals (top: room temperature; bottom: 77 K).

Table 5. Base metal Charpy tests

Material	Condition	Temperature (°C)	Orientation	Energy (ft-lb)	
Ring	Forging	22	TL	>240	
		-196		86	
					138
					84
					123
		Gleebled	22		>300
		-196		175	
				177	
1-in. plate	Not known	22	TL	251	
			TS	284	
		-196	TL	70	
				77	
			TS	74	
				76	
		Gleebled	22	TL	>300
			-196		90
					86
	4-in. plate	Quenched	22	TL	295
-196			84		
					83
		Quenched and Gleebled	22		>300
			-196		26 <sup>a</sup>
					101
		Hot rolled	22		272
			-196		64
					74
		Hot rolled and Gleebled	22		>300
		-196		94	
				101	
7-in. plate	Quenched	22	TL	>300	
		-196		102	
					76
		Quenched and Gleebled	22		>300
			-196		105
					126
		Hot rolled	22		227
					232
			-196		39
					31
	Hot rolled and Gleebled	22		>300	
		-196		55	
				42	

<sup>a</sup>Examination of the fracture surface indicated that the specimen had been overheated during the Gleeble simulation. This produced a hot crack that was responsible for the very low energy level.

Table 6. Weld metal Charpy tests

Material	Temperature (°C)	Orientation	Energy (ft-lb)	
Nitronic 40W	22	TL	126	
		TS	132 123 115	
	-196	TL	6	
		TS	7 5 8	
	Nitronic 35W	22	TL	113
			TS	132 113 133
-196		TL	8	
		TS	14 17 12	
Type 21-6-9 filler		22	TL	158
			TS	154 139 146
	-196	TL	13	
		TS	19 27 24	
	Inconel 625	22	TL	26
			TS	25 31 25
-196		TL	15	
		TS	15 16 18	
Inconel 625 PLUS		22	TL	57
			TS	55 56 53
	-196	TL	39	
		TS	39 43 42	
	Inconel 82	22	TL	150
			TS	107 137 105
-196		TL	135	
		TS	121 121 94	
Inconel 182		22	TL	102
			TS	104 89 87
	-196	TL	81	
		TS	89 80 77	

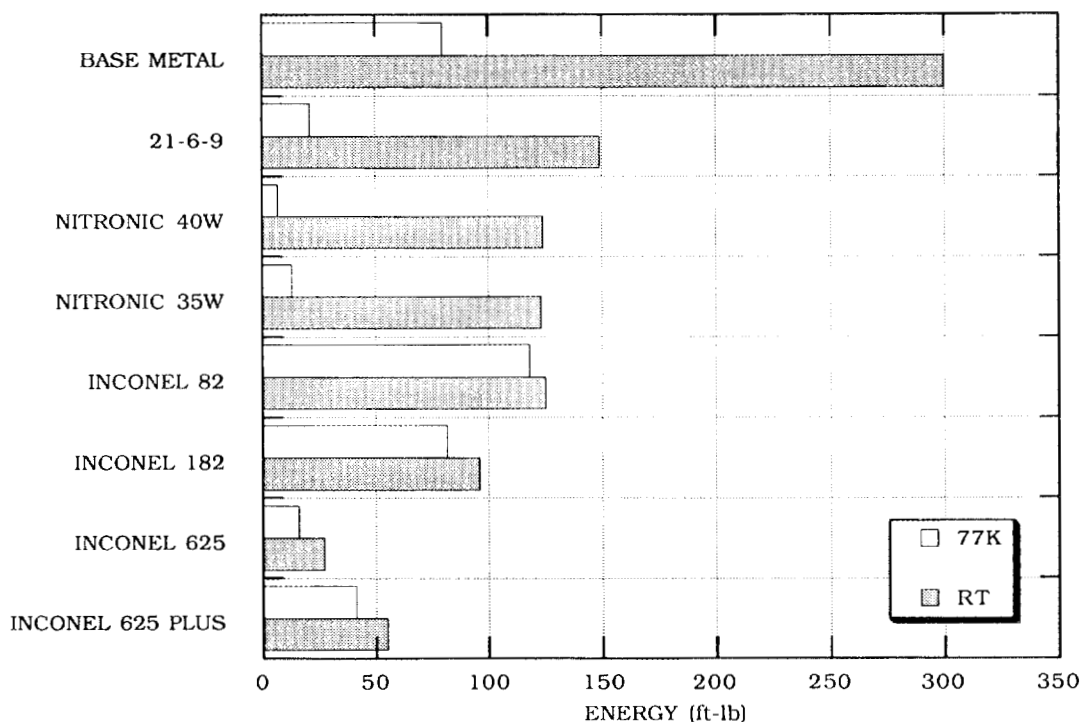


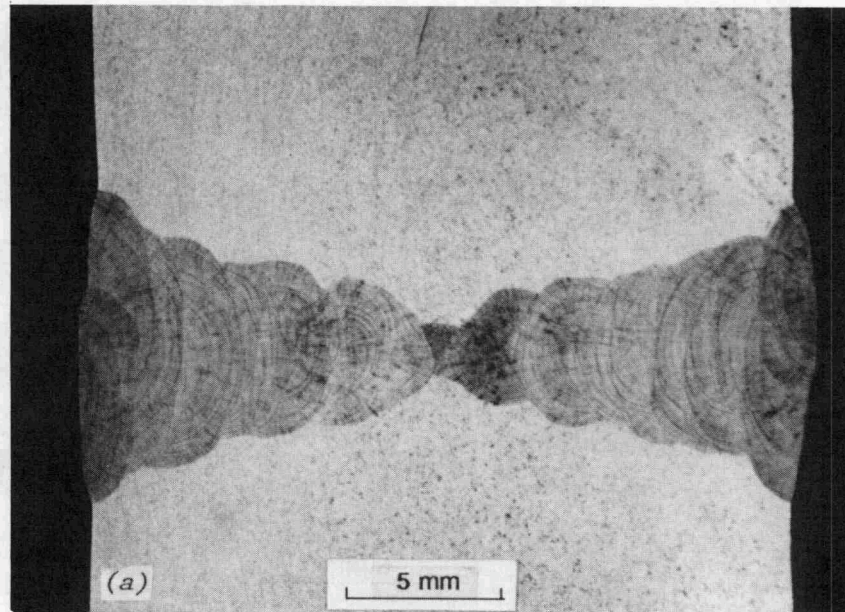
Fig. 4. A comparison of the average Charpy impact energies for the type 21-6-9 base metals and the weld filler metals at room temperature and at 77 K.

properties were very poor except for the Inconel 82 and 182 alloys. These alloys had excellent impact properties at both temperatures, particularly Inconel 82.

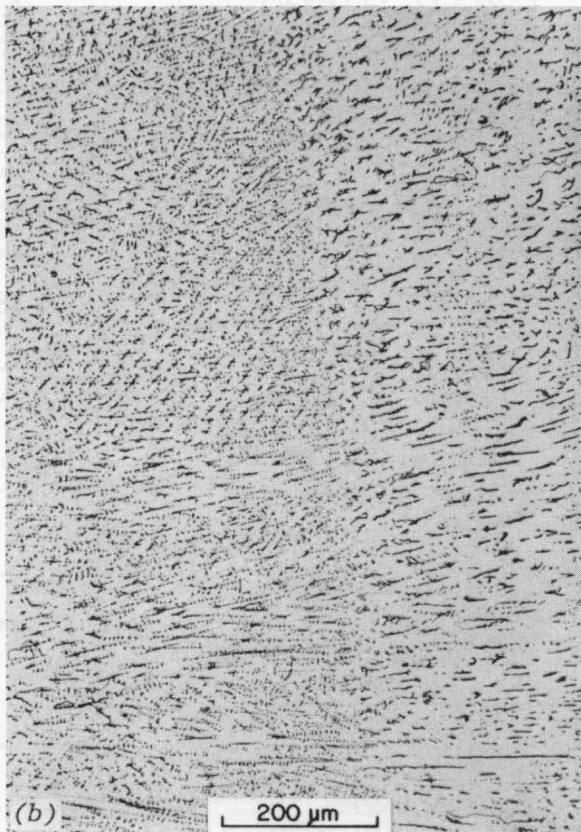
The impact specimens that had absorbed large amounts of energy showed greatly distorted fracture surfaces and extensive plasticity. The low-energy specimens were much less distorted. The Nitronic specimens showed a change in fracture appearance from a ductile, distorted fracture appearance at room temperature to a much flatter, brittle appearance at 77 K. The Inconel 625 specimens showed evidence of porosity on the fracture surface. These voids were quite large [i.e., typically 0.5 mm in diameter (0.020 in.)].

Figures 5 through 11 show the microstructures of the different weld metals. Figure 5 shows the type 21-6-9 filler metal (i.e., weld G25); Fig. 6, the Nitronic 40W (i.e., weld G17); and Fig. 7, the Nitronic 35W

Y217087



Y217088



Y217089

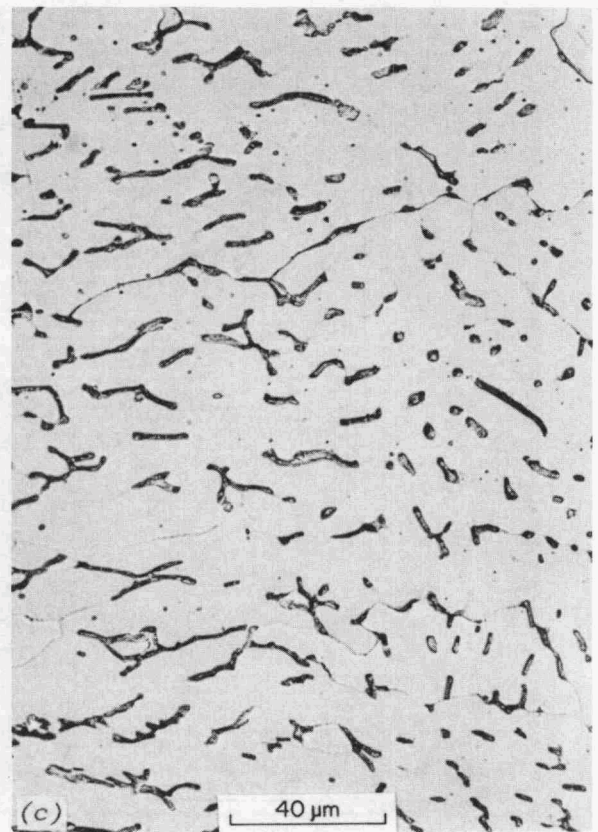
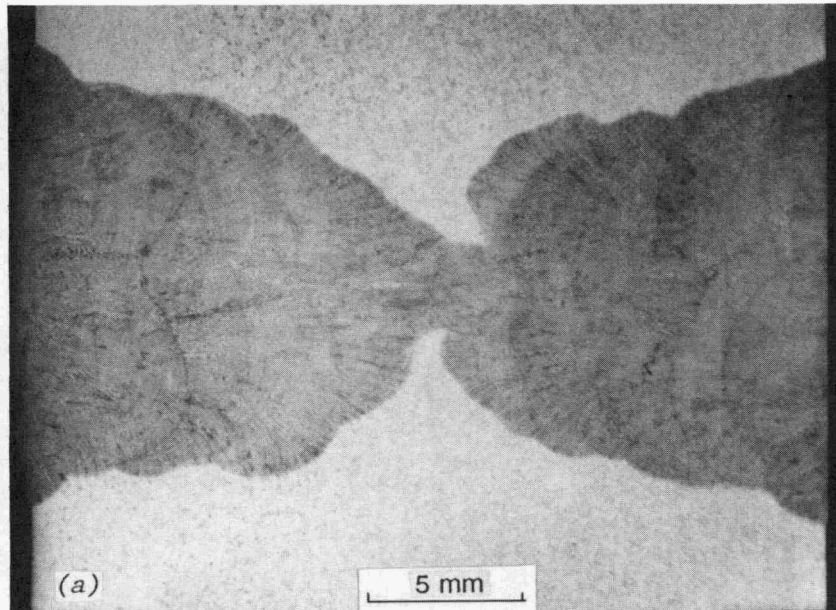
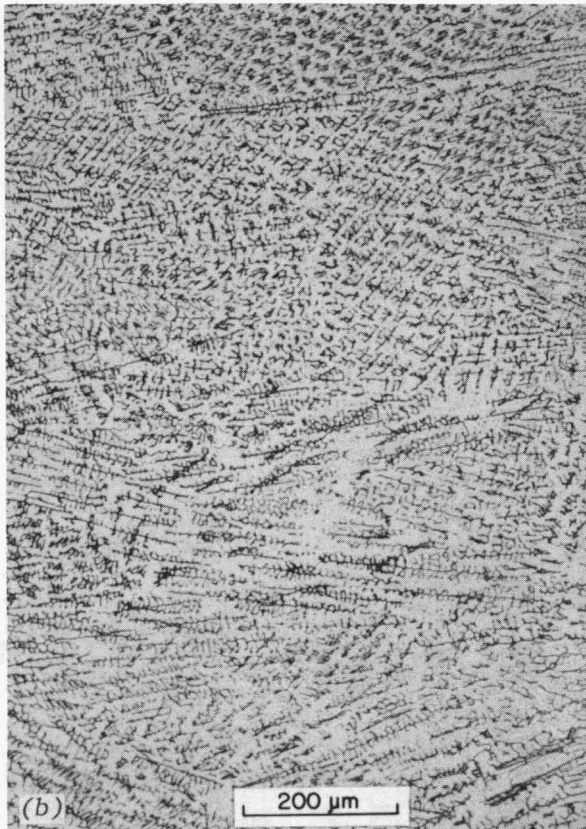


Fig. 5. Weld G25 with type 21-6-9 filler metal: (a) macroscopic view of weld, (b) low-magnification view of weld metal, and (c) higher magnification view showing ferrite phase in an austenitic matrix.

Y216484



Y216486



Y216496

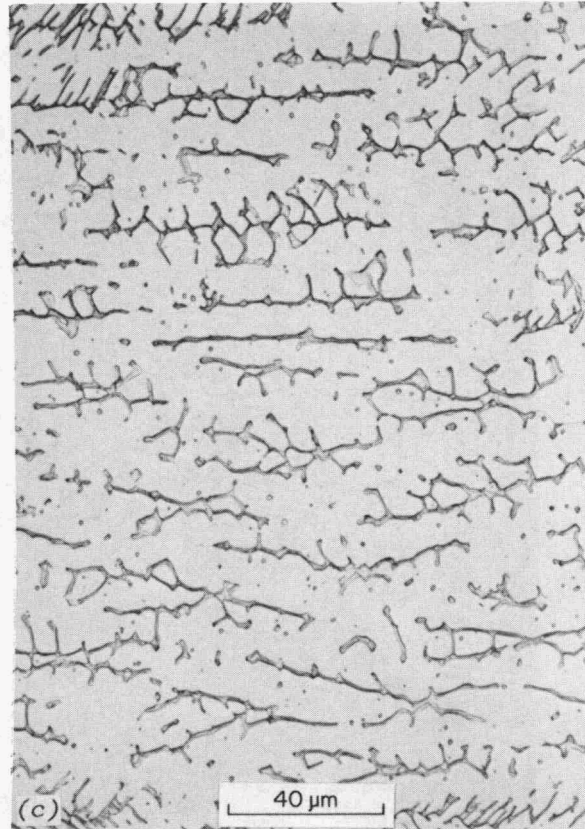
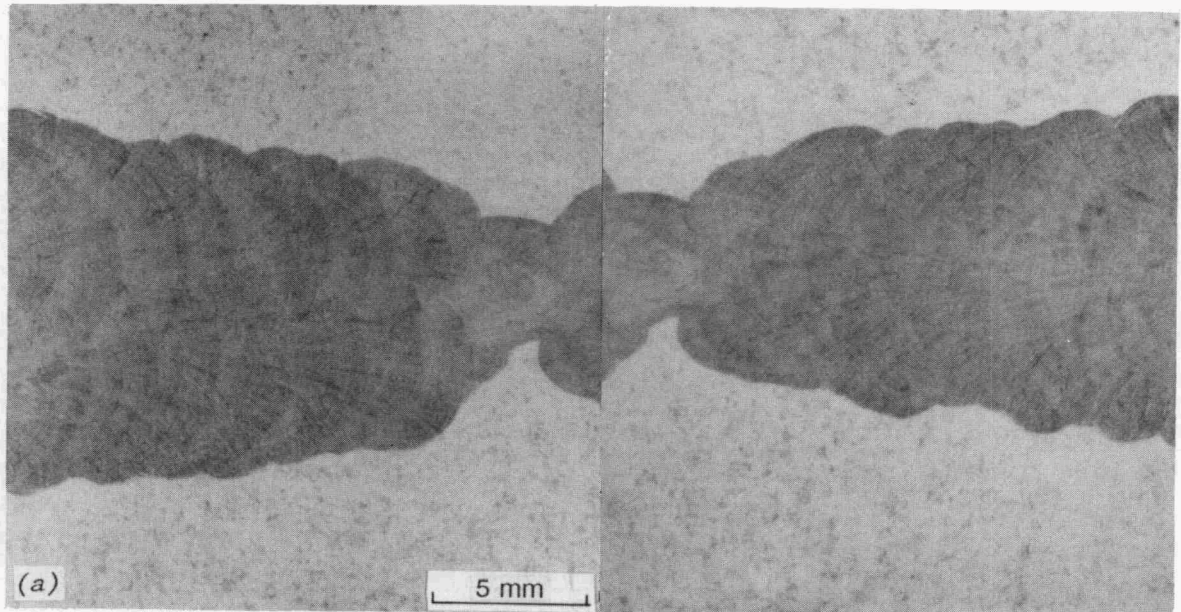


Fig. 6. Weld G17 with Nitronic 40W filler metal: (a) macroscopic view of weld, (b) low-magnification view of weld metal, and (c) higher magnification view showing ferrite phase in an austenitic matrix.

Y216421

Y216422



Y216428

Y216431

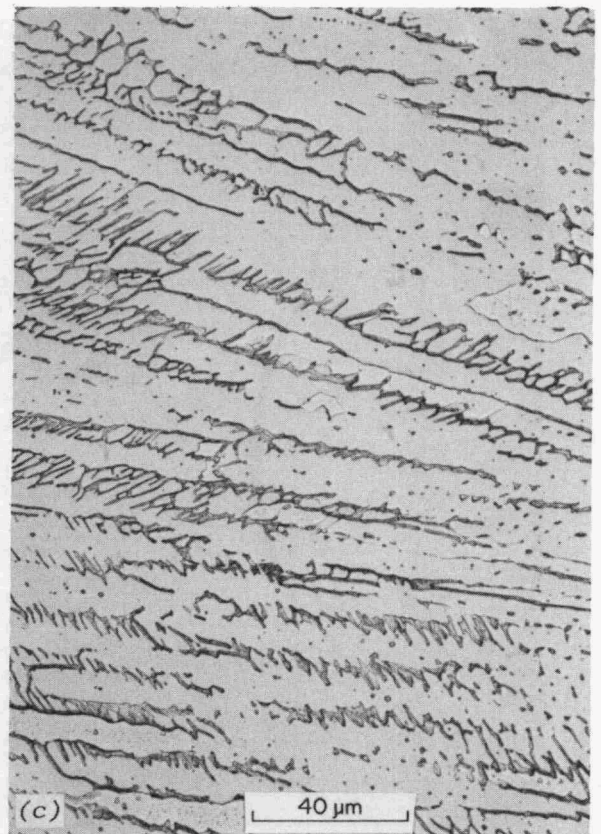
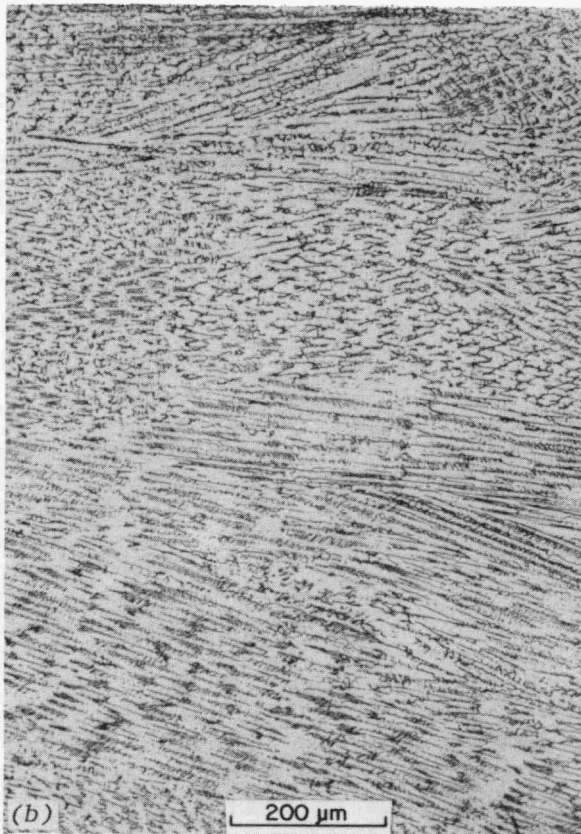
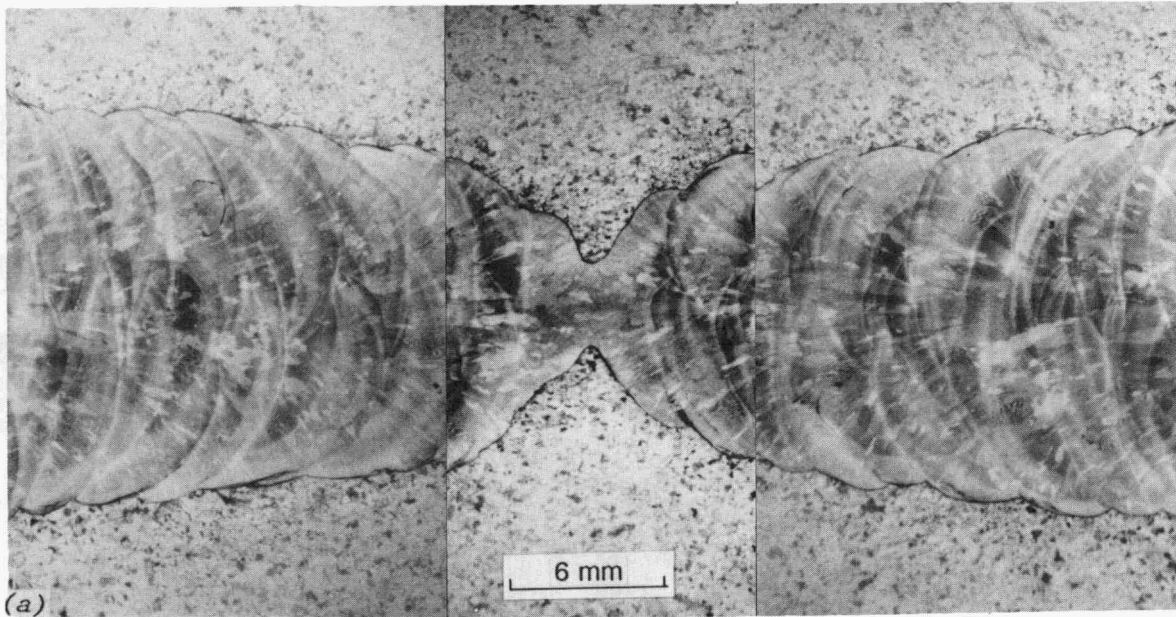


Fig. 7. Weld G20 with Nitronic 35W filler metal: (a) macroscopic view of weld, (b) low-magnification view of weld metal, and (c) higher magnification view showing ferrite phase in an austenitic matrix.

Y216571

Y216573

Y216572



Y216577

Y216584

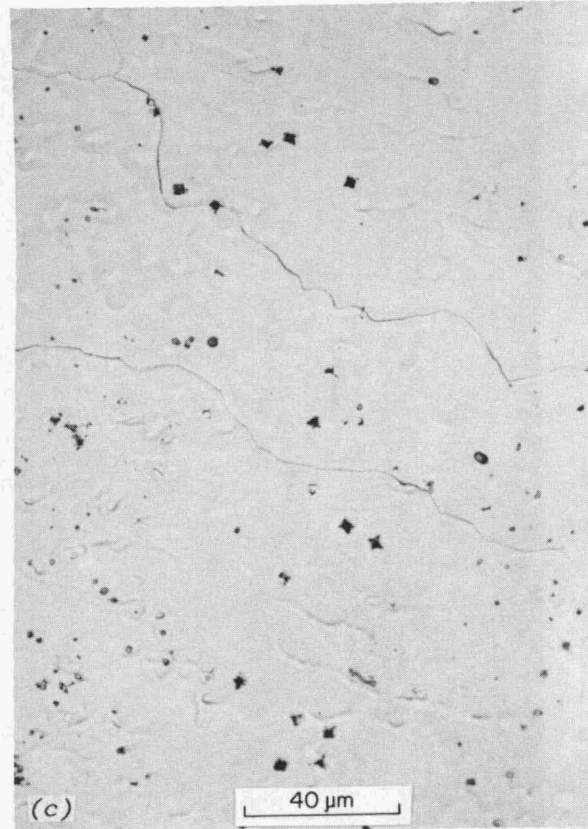
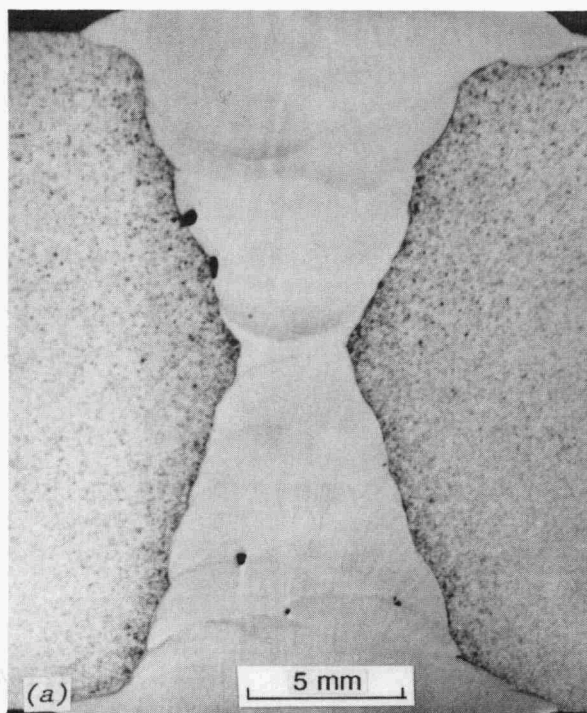


Fig. 8. Weld G19 with Inconel 82 filler metal: (a) macroscopic view of weld, (b) low-magnification view of weld metal showing isolated porosity and lack of fusion in the weld metal, and (c) higher magnification of weld metal showing fully austenitic weld.

Y217094

Y217097



Y217098

Y217095

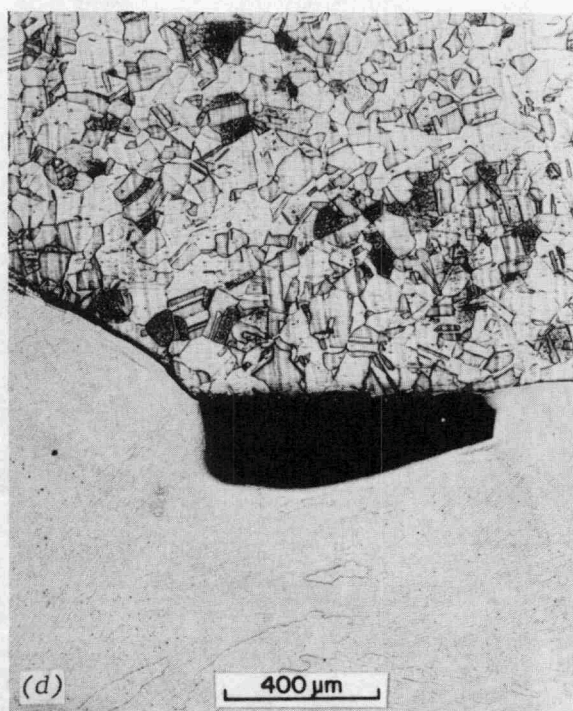
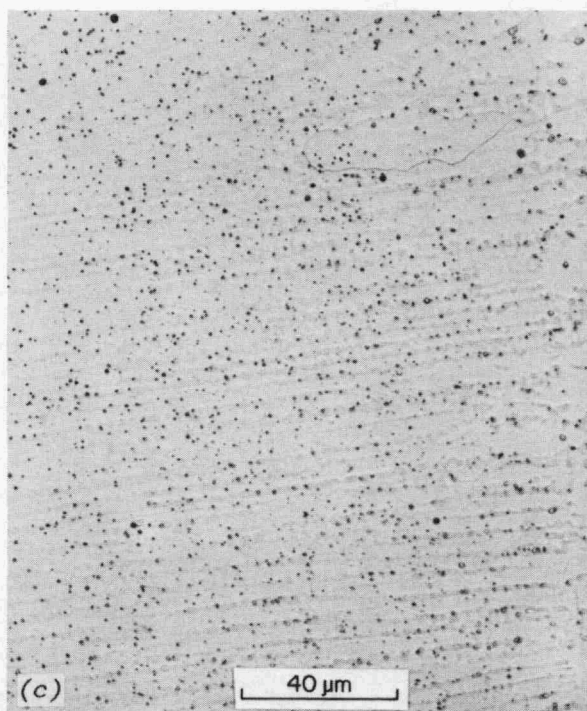
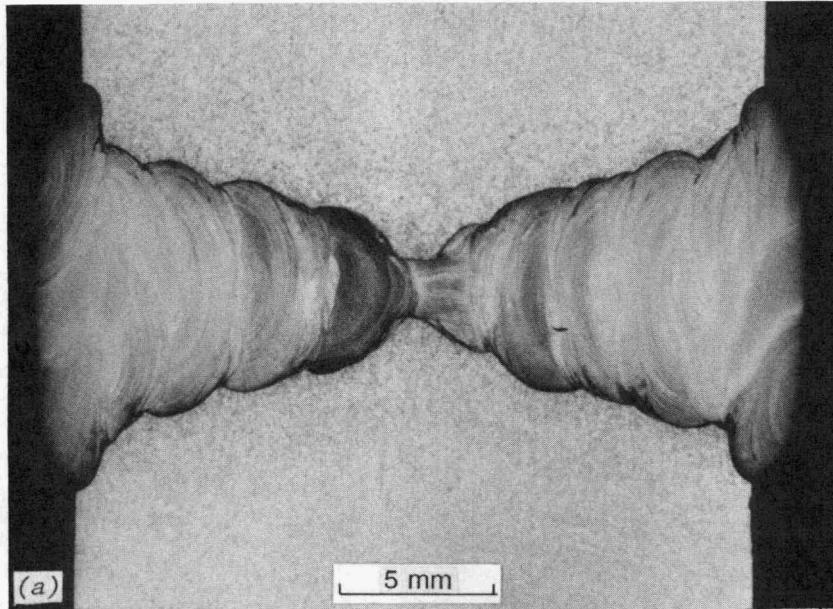
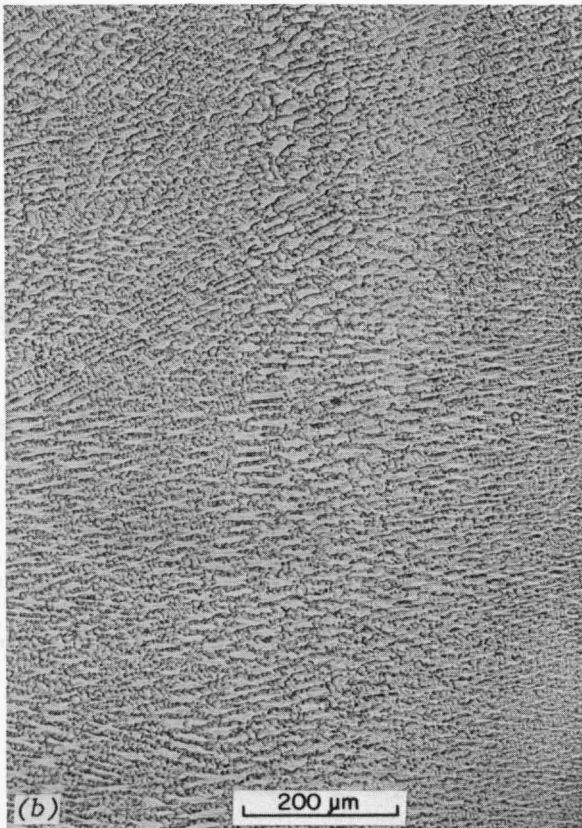


Fig. 9. Weld G28 with Inconel 182 filler metal: (a) macroscopic view of weld, (b) low-magnification view of weld metal, (c) higher magnification view, and (d) view of edge of weld showing lack of fusion at fusion line.

Y216474



Y216479



Y216483

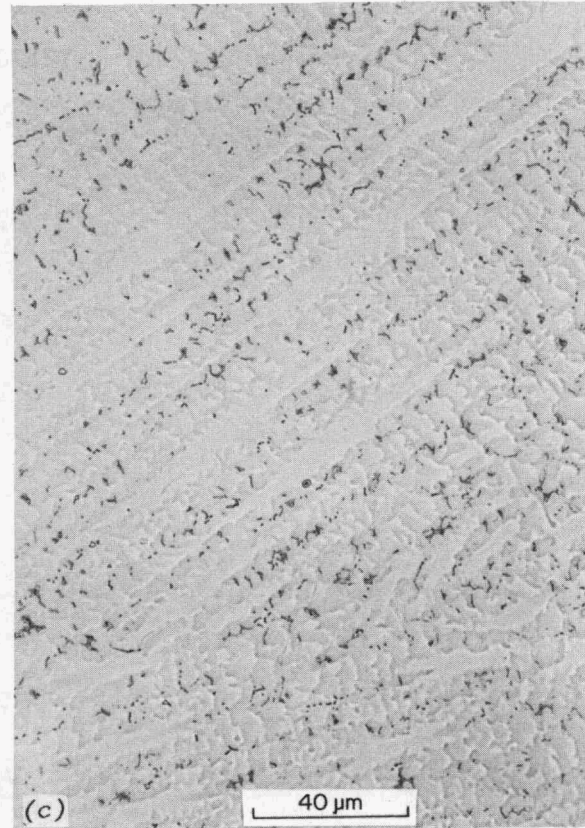
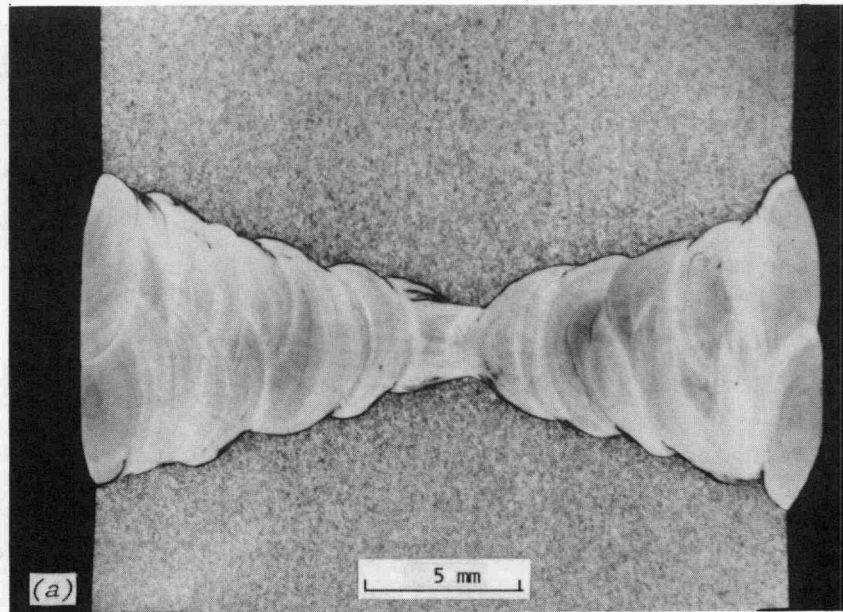
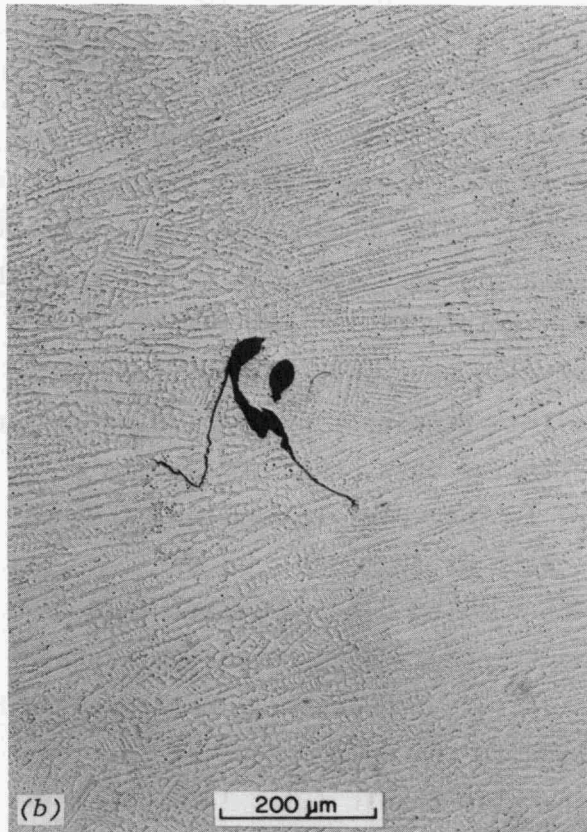


Fig. 10. Weld G18 with Inconel 625 filler metal: (a) macroscopic view of weld, (b) low-magnification view of weld metal, and (c) higher magnification of weld metal showing fully austenitic weld.

Y217090



Y217091



Y217093

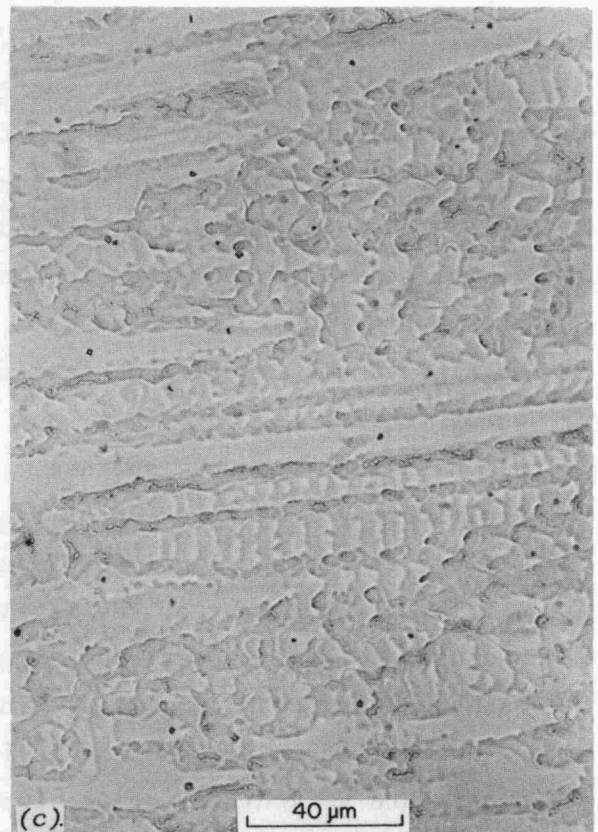


Fig. 11. Weld G27 with Inconel 625 PLUS filler metal: (a) macroscopic view of weld, (b) low-magnification view of weld metal showing lack of fusion in the weld metal, and (c) higher magnification of weld metal showing fully austenitic weld.

(i.e., weld G20). All these filler metals contain a significant amount of ferrite phase in a predominantly austenitic matrix. Figures 8 through 11 show the Inconel-type filler metals (i.e., nickel-based alloys that do not contain ferrite). Figure 8 shows the Inconel 82 filler (i.e., weld G19); Fig. 9, the Inconel 182 (i.e., weld G28); Fig. 10, the Inconel 625 (i.e., weld G18); and Fig. 11, the Inconel 625 PLUS (i.e., weld G27). Figure 12 shows the base metal and HAZs.

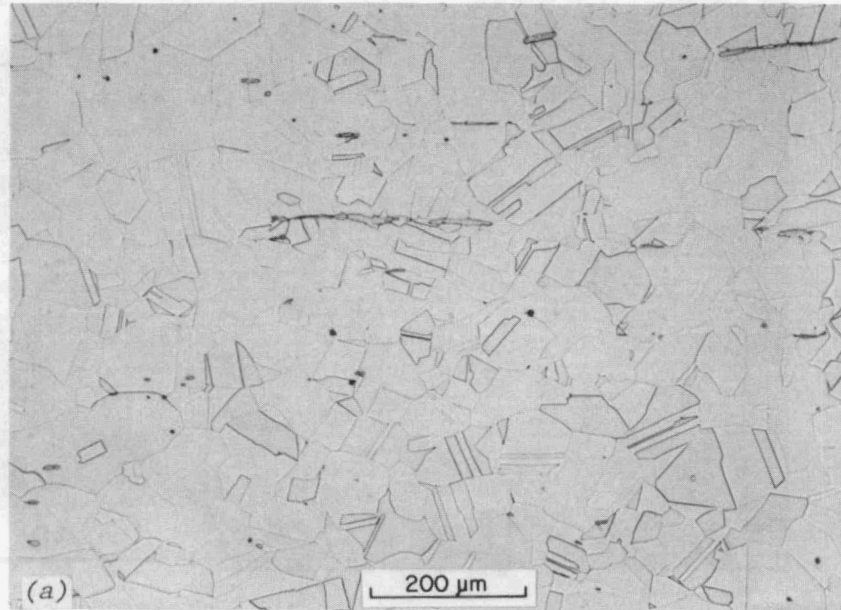
## DISCUSSION

The testing conducted in Phase I produced several interesting results. The Nitronic-type filler metals have high strengths but suffer a severe decrease in impact energy at lower temperature. The Inconel alloys are slightly weaker than the Nitronic alloys at room temperature and much weaker at 77 K. The Inconel 82 and 182 alloys offer good impact properties—the Inconel 82 alloy being both stronger and tougher at all temperatures. The Inconel 625 PLUS and, particularly, the Inconel 625 filler metal have low impact energies regardless of temperature.

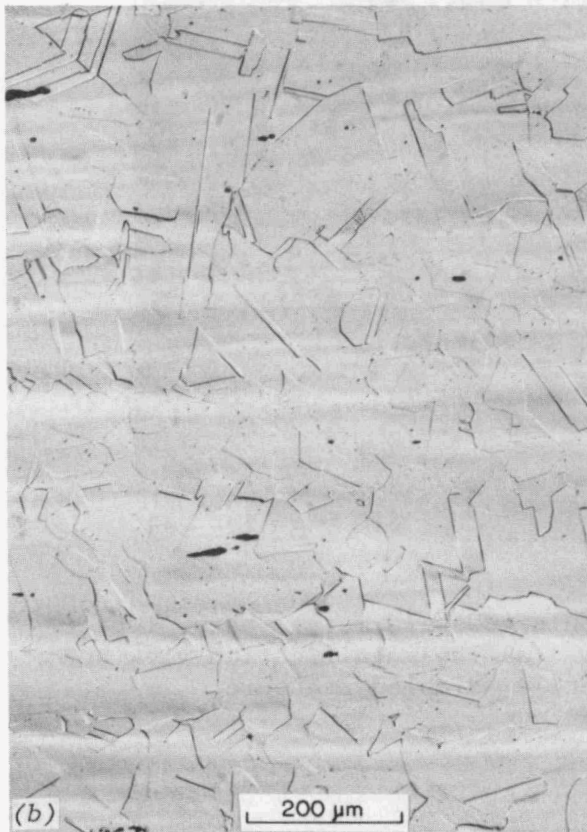
The microstructure of the Nitronic-type filler metals offers an explanation for the dramatic decrease in energy absorbed as the temperature is lowered. The welds contain about 10% ferrite phase (see Figs. 5 through 7), which is also reflected in their slight magnetism. It is believed that this ferrite phase fractures by a cleavage process at low temperatures. The high-volume fraction of ferrite permits the crack to move readily to nearby ferrite regions; thus, the fracture process requires low energy and creates a flat fracture surface. Any filler metal that results in a significant volume fraction of ferrite in the weld will probably show a similar, low energy level for impact tests at 77 K.

The fractography of the ferrite-containing welds supports this conclusion. Fracture at room temperature occurs by a ductile microvoid coalescence process (Fig. 13). This fracture process will be dominated by the austenitic matrix and the inclusions in the weld. However, at low temperature very different fracture features result (Fig. 14). The fracture surface consists of flat steps that are linked by narrow ridges of ductile tearing. The crack seems to preferentially follow the ferrite

Y216494



Y216424



Y216423

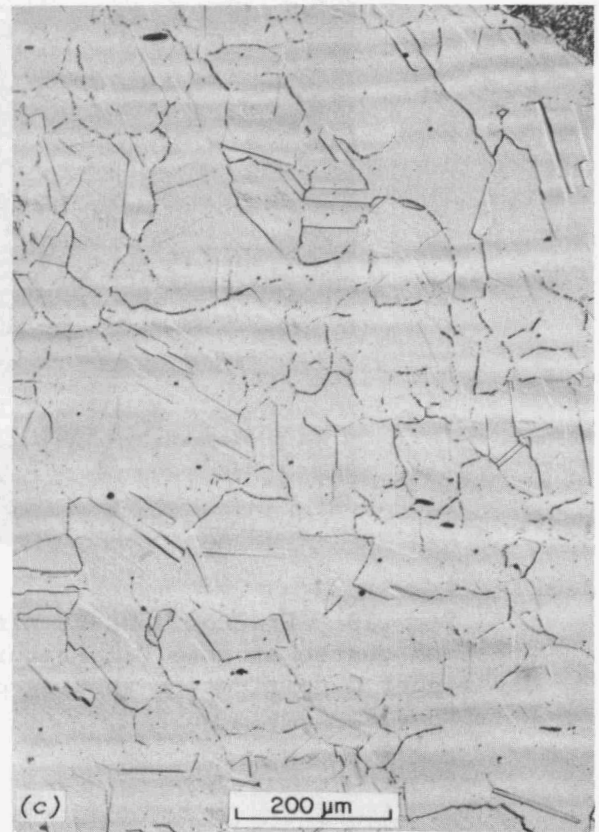
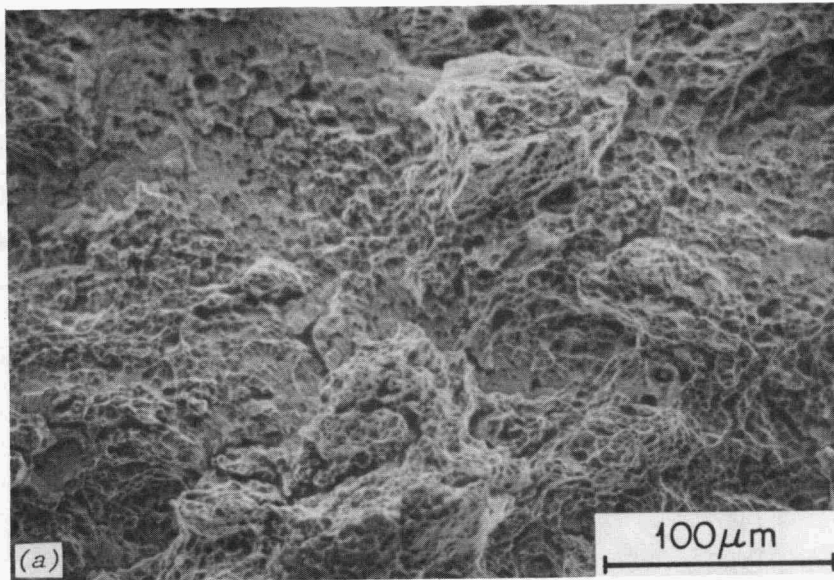


Fig. 12. Type 21-6-9 base metal: (a) base metal from forging from weld G17 (note austenitic matrix with twins in grains and occasional regions of ferrite), (b) base metal from 100-mm plate from weld G20, and (c) heat-affected zone from weld G20 (note fine structure in austenite grains and coarser carbides on grain boundaries near weld fusion line).

M30373



M30374

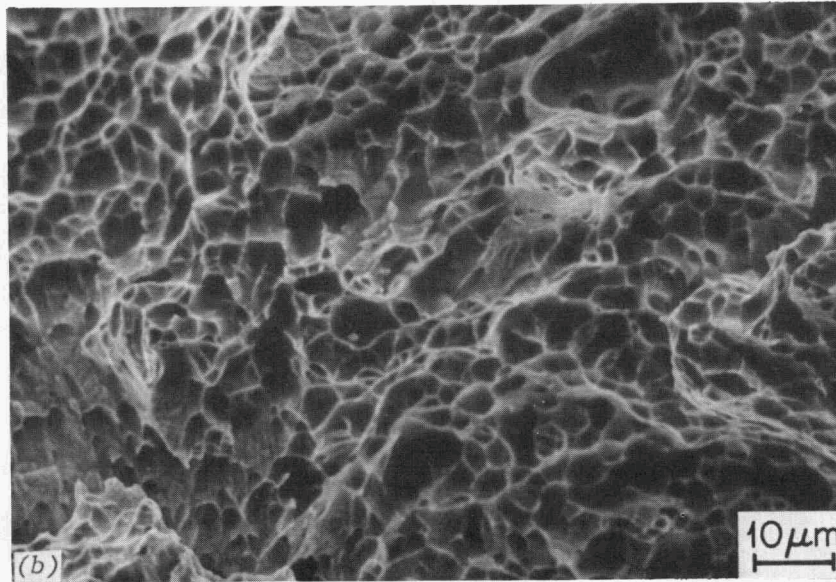
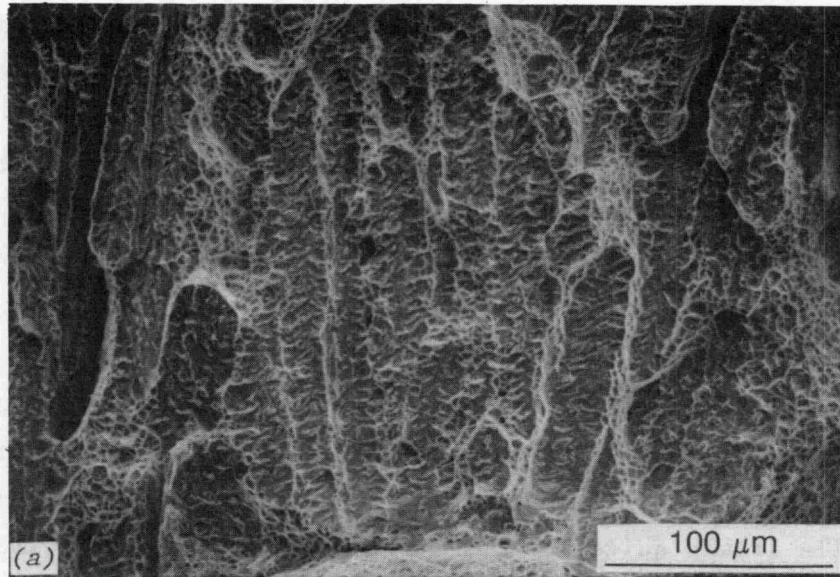


Fig. 13. Fractographs of Nitronic 40W weld metal Charpy impact specimen tested at room temperature: (a) low-magnification view and (b) higher magnification showing ductile, dimpled fracture.

M30370



M30372

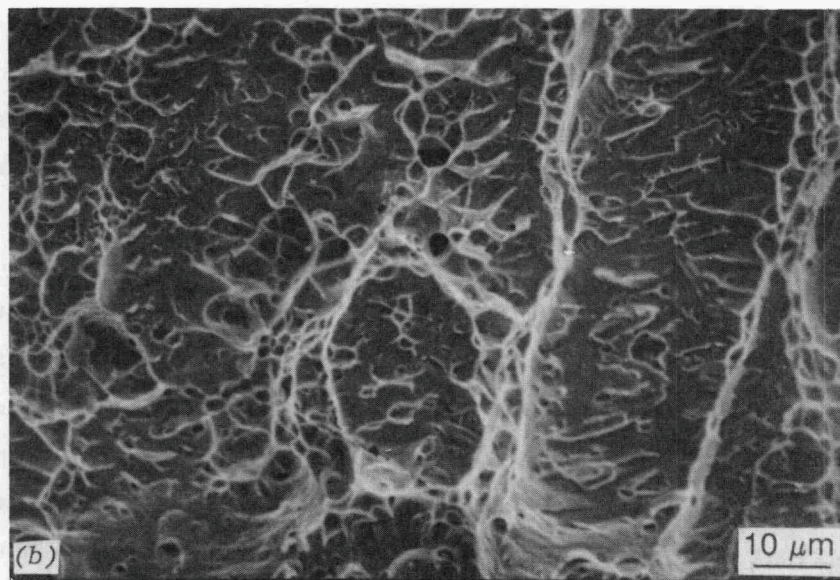


Fig. 14. Fractographs of Nitronic 40W weld metal Charpy impact specimen tested at 77 K: (a) low-magnification view showing stepped surface and (b) higher magnification showing flat regions joined by tear ridges.

phase and jumps from one island of ferrite to another. The flat regions are the result of cleavage fracture of the ferrite phase, while the tearing results from crack joining these areas together by ductile tearing of the austenite matrix between the ferrite.

The Inconel alloys do not contain any ferrite phase in their weld metal. These alloys create a fully austenitic weldment (see Figs. 8 through 11) as is indicated by their total lack of magnetism. The austenitic microstructure is not susceptible to cleavage fracture; thus, the fracture process is ductile at either test temperature. These welds did contain welding defects [Figs. 8(b), 9(d), and 11(b)] that are related to the high nitrogen content of the base metal (noted earlier). Despite such defects, the impact energy of the Inconel 82 and 182 welds was quite high, while it was quite low for the Inconel 625 and 625 PLUS materials.

The Inconel 82 filler metal is clearly the best of the alloys examined to date. It offers excellent impact properties over the temperature range of interest, and it provides reasonable strength. It exceeds the base metal strength at room temperature but falls below the base metal strength at 77 K. The severity of this possible restriction on the vessel design is not clear. Possibly, the yield strength may be increased through composition modifications, resulting in some decrease in the impact properties.

The type 21-6-9 base metal (Fig. 12) is primarily austenitic; occasionally, twins occur. Small amounts of ferrite were observed [Fig. 12(b)] but had little effect on the low-temperature impact toughness. The HAZ contained evidence of deformation [Fig. 12(c)] presumably induced by the welding process. It is not known if these are twins or slip bands. This, together with the coarsened carbides noted at grain boundaries [Fig. 12(c)], may explain why the HAZ was stronger than the base metal in the oversize tensile specimens.

## CONCLUSIONS

Seven different filler metals have been used to produce weldments in thick sections in type 21-6-9 stainless steel plate and forging. Tensile and Charpy impact tests were performed at room temperature and at 77 K.

These tests indicate that the Nitronic-type filler metals (which contain a significant fraction of ferrite) have strengths that exceed the base metal but have very low impact energies at 77 K. The Inconel-type filler metals (which do not contain ferrite) are somewhat weaker than the base metal. The Inconel 82 and 182 filler metals offer good impact properties at both temperatures but are weaker than the base metal at 77 K. The Inconel 625 and 625 PLUS materials have relatively poor impact properties. Based on these test results, the authors believe that the Inconel 82 filler metal is the prime candidate material for welding type 21-6-9 stainless steel in thick sections.

#### ACKNOWLEDGMENTS

The authors express their appreciation to John Citrolo and the Princeton Plasma Physics Laboratory staff for their support and helpful comments; to J. D. McNabb of the Materials Joining Group at Oak Ridge National Laboratory for fabrication of the welds; to E. T. Manneschildt, J. J. Henry, Jr., and M. J. Swindeman for the mechanical testing; to M. L. Santella, R. L. Klueh, and R. K. Nanstad for their helpful reviews; to J. L. Bishop and K. W. Gardner for preparation of the manuscript; and to D. L. Balltrip and S. M. Wilson for preparation of the final document.

## BIBLIOGRAPHY

1. R. H. Espy, "Weldability of Nitrogen Strengthened Stainless Steels," *Weld. J.* 61(5), 140s-56s (1982).
2. J. A. Brooks, "Weldability of High N, High Mn Austenitic Stainless Steel," *Weld. J.* 54(6), 189s-95s (1975).
3. M. J. Cieslak, T. J. Headley, and R. B. Frank, "The Welding Metallurgy of Custom Age 625 PLUS Alloy," *Weld. J.* 68(12), 473s-82s (1989).
4. C. E. Witherell, "Welding Stainless Steels for Structures Operating at Liquid Helium Temperature," *Weld. J.* 59(11), 326s-42s (1980).
5. W. A. Logsdon et al., *Material Evaluation and Selection for Superconducting Magnet Sheathing-Large Coil Program*, Westinghouse Electric Corp., R&D Center, Pittsburgh, Pa.
6. G. M. Goodwin, "Welding Process Selection for Fabrication of a Superconducting Magnet Structure," *Weld. J.* 64(8), 19-26 (1985).
7. H. Nakajima et al., "Mechanical Properties of Welded Joints of the New Cryogenic Steel," in *9th Annual Cryogenic Structural Materials Workshop, October 6-8, 1986, Reno, Nevada*, Natl. Bureau of Standards, Washington, D.C., 1986.
8. E. R. Szumachowski and H. F. Reid, "Cryogenic Toughness of SMA Austenitic Stainless Steel Weld Metal: Part I, Role of Ferrite," *Weld. J.* 57(11), 325s-33s (1978).
9. E. R. Szumachowski and H. F. Reid, "Cryogenic Toughness of SMA Austenitic Stainless Steel Weld Metal: Part II, Role of Nitrogen," *Weld. J.* 58(2), 34s-44s (1979).
10. R. H. Espy, "Evaluation of Weld Fillers to Join Nitrogen Strengthened Austenitic Stainless Steels for Cryogenic Applications," pp. 455-63 in *Materials Studies for Magnetic Fusion Energy Applications at Low Temperature - IV*, NBSIR 81-1645, Natl. Bureau of Standards, Washington, D.C., 1981.
11. R. L. Tobler et al., "Tensile, Fatigue and Fracture Properties of an Fe-18Cr-16Ni-6.5Mn-2.4Mo Fully Austenitic SMA Weld at 4 K," pp. 257-76 in *Materials Studies for Magnetic Fusion Energy Applications at Low Temperature - IX*, NBSIR 86-3050, Natl. Bureau of Standards, Washington, D.C., 1986.

12. C. N. McCowan, T. A. Siewert, and R. L. Tobler, "Tensile and Fracture Properties of an Fe-18Cr-10Ni-5Mn-0.16N Fully Austenitic Weld Metal at 4 K," pp. 247-56 in *Materials Studies for Magnetic Fusion Energy Applications at Low Temperature - IX*, NBSIR 86-3050, Natl. Bureau of Standards, Washington, D.C., 1986.

13. T. Matsumoto et al., "Mechanical Properties of Fully Austenitic Weld Deposits for Cryogenic Structures," *Weld. J.* 66(4), 120s-26s (1987).



## INTERNAL DISTRIBUTION

1-2.	Central Research Library	41.	M. K. Miller
3.	Document Reference Section	42.	R. K. Nanstad
4-5.	Laboratory Records Department	43.	R. W. Reed, Jr.
6.	Laboratory Records, ORNL RG	44.	M. J. Saltmarsh
7.	ORNL Patent Section	45.	M. L. Santella
8-10.	M&C Records Office	46.	T. E. Shannon
11-15.	D. J. Alexander	47.	J. Sheffield
16.	K. B. Alexander	48.	G. M. Slaughter
17-21.	E. E. Bloom	49.	J. O. Stiegler
22.	D. R. Childress	50.	R. W. Swindeman
23.	W. R. Corwin	51.	A. W. Trivelpiece
24.	D. F. Craig	52.	J. M. Vitek
25-28.	S. A. David	53.	F. W. Wiffen
29-33.	G. M. Goodwin	54.	T. Zacharia
34.	M. L. Grossbeck	55.	A. D. Brailsford (Consultant)
35.	F. M. Haggag	56.	Y. A. Chang (Consultant)
36.	C. R. Hubbard	57.	H. W. Foglesong (Consultant)
37.	J. F. King	58.	J. J. Hren (Consultant)
38.	M. S. Lubell	59.	M. L. Savitz (Consultant)
39.	J. R. Mayotte	60.	J. B. Wachtman, Jr. (Consultant)
40.	P. J. Maziasz		

## EXTERNAL DISTRIBUTION

61. ALLEGHENY LUDLUM STEEL, Division of Allegheny Ludlum Corporation,  
Technical Center, Brachenridge, PA 15014-1597  
J. F. Grubb, Ph.D.
62. CARPENTER TECHNOLOGY CORPORATION, P.O. Box 14662, Reading, PA  
19612-4662  
R. S. Brown, Product Application Manager
63. WELDING RESEARCH COUNCIL, 345 East 47th Street, Suite 1301,  
New York, NY 10017  
Dr. M. Prager

64. DOE, Assistant Secretary for International Affairs and Energy  
Emergencies (IE-1), Washington, DC 20585  
J. J. Easton, Jr.
- 65-69. DOE, FUSION ENERGY, Office of Energy Research, Washington DC 20585  
N. A. Davies, Acting Associate Director  
J. Decker, Acting Director  
R. J. Dowling  
R. E. Price  
F. W. Wiffen
70. DOE/FIELD OFFICE, Oak Ridge, TN 37831-6269  
Office of Assistant Manager for Energy Research and  
Development
- 71-110. DOE, OFFICE OF SCIENTIFIC AND TECHNICAL INFORMATION, P.O. Box 62,  
Oak Ridge, TN 37831  
For distribution as shown in DOE/OSTI-4500-R75,  
Distribution Category UC-424 (Magnetic Fusion  
Energy Systems).